Structural and Electronic Characteristics of the Monoboro-Analogs of the Acetylcholine Cation As Determined by the Semiempirical MNDO Computational Method

Michael A. Egan and Robert W. Zoellner*

Department of Chemistry, Northern Arizona University, P.O. Box 5698, Flagstaff, Arizona 86011-5698

Received September 14, 1992

The semiempirical computational method MNDO (modified neglect of diatomic overlap) has been used to calculate the stable conformations and the electronic properties of each of the five possible monoboro-analogs of the acetylcholine cation, **ACH**$^+$. The thermodynamically most stable analog was determined to be $(CH_3)_3NBH_2CH_2OC(O)CH_3$, the 5-boro-analog, **5**, *not* the commercially-available isomer (7-boroacetylcholine, $H_3BN(CH_3)_2CH_2CH_2OC(O)CH_3$, **7**). In addition, the relative Boltzmann distribution populations of the minimum-energy conformations of each analog, as defined by the torsion angles O^3–C^4–C^5–N^6 and C^2–O^3–C^4–C^5, were determined. From the conformational energy maps produced by these torsion angles, the 4-boro-analog, $(CH_3)_3NCH_2BH_2OC(O)CH_3$, **4**, and **7** appear to exhibit the most similarities to **ACH**$^+$ in the number and the geometries of accessible conformations. Because the monoboro-analogs of **ACH**$^+$ are zwitterionic neutral molecules, while **ACH**$^+$ is cationic, few direct electronic comparisons could be drawn. However, molecules exhibiting regional electronic distributions (such as the overall charge on the cationic head) which are similar to those of **ACH**$^+$ are identified and discussed.

Introduction

We have developed an interest in the structure and the electronic properties of the acetylcholine cation (**ACH**$^+$), $[(CH_3)_3NCH_2CH_2OC(O)CH_3]^+$, as compared to (2-acetoxyethyl)dimethylamine–borane, its isoelectronic and reportedly[1] isostructural monoboro-analog, $H_3BN(CH_3)_2CH_2CH_2OC(O)CH_3$, **7**. The relatively simple synthesis of this molecule[1] and other boro derivatives of biological molecules[2-6] has led to an increased interest in their pharmacological activities.[7,8]

In addition to **7**, which is commercially-available, four other monoboro-analogs of **ACH**$^+$ can be envisioned (see Chart I). The monoboro-analogs of **ACH**$^+$ are zwitterionic, neutral molecular species, whereas **ACH**$^+$ is cationic. The tetravalent boron atom in the monoboro-analogs carries a formal negative charge which balances the formal positive charge on the tetravalent nitrogen atom. This fundamental difference in charge will undoubtedly play an important role in the physical and chemical properties of the monoboro-analogs of **ACH**$^+$ and may effect the mechanisms through which the molecules interact with biological systems.

Due to the important role **ACH**$^+$ plays in the transmission of nerve impulses, extensive conformational studies have been conducted using X-ray diffraction techniques[9-20] as well as by Raman spectroscopic,[21] electron diffraction,[22] and NMR[23-27] techniques. Of particular importance is the ability of **ACH**$^+$ to bind to receptors of the postsynaptic membrane and the eventual degradation of **ACH**$^+$ by acetylcholinesterase (**ACHase**), two processes highly dependant upon overall molecular conformation.

The results reported herein detail the computationally-derived stable conformations of each of the five possible neutral monoboro-analogs of **ACH**$^+$ as determined by the semiempirical MNDO (modified neglect of diatomic overlap) method. The calculated structures and atomic charge distributions of these monoboro-analogs are compared to the experimental and calculated structures and atomic charge distributions of the conformations of **ACH**$^+$. These results were previously reported in preliminary form.[28]

Computational Methods

All MNDO calculations were performed using Quantum Chemistry Program Exchange program no. 455, version 5.0,[29] running on Apollo/Hewlett-Packard Domain Series DN3550 and

(1) Spielvogel, B. F.; Ahmed, F. U.; McPhail, A. T. *J. Am. Chem. Soc.* **1986**, *108*, 3824.
(2) Spielvogel, B. F.; Ahmed, F. U.; McPhail, A. T. *Inorg. Chem.* **1986**, *25*, 4395.
(3) Malone, L. J.; Parry, R. W. *Inorg. Chem.* **1967**, *6*, 817.
(4) Koehler, K. A.; Hess, G. P. *Biochemistry* **1974**, *13*, 5345.
(5) Mancilla, T.; Santiesteban, F.; Contreras, R.; Klaebe, A. *Tetrahedron Lett.* **1982**, *23*, 1561.
(6) Brown, H. C.; Murray, L. T. *Inorg. Chem.* **1984**, *23*, 2746.
(7) Hall, I. H.; Spielvogel, B. F.; Sood, A. *Anti-Cancer Drugs* **1990**, *1*, 133.
(8) Sood, A.; Sood, C. K.; Spielvogel, B. F.; Hall, I. H.; Wong, O. T.; Mittakanti, M.; Morse, K. *Arch. Pharm.* **1991**, *324*, 423.
(9) Sörum, H. *Acta Chem. Scand.* **1959**, *13*, 345.
(10) Canepa, F. G.; Pauling, P.; Sörum, H. *Nature (London)* **1966**, *210*, 907. (The results in this reference have been reinvestigated and are superceded by the results in ref 18.)
(11) Shefter, E.; Kennard, O. *Science (Washington, D.C.)* **1966**, *153*, 1389.
(12) Chothia, C.; Pauling, P. *Nature (London)* **1968**, *219*, 1156.
(13) Herdklotz, J. K.; Sass, R. L. *Biochem. Biophys. Res. Commun.* **1970**, *40*, 583.
(14) Mahajan, V.; Sass, R. L. *J. Cryst. Mol. Struct.* **1974**, *4*, 15.
(15) Marzotto, A.; Graziani, R.; Bombieri, G.; Forsellini, E. *J. Cryst. Mol. Struct.* **1974**, *4*, 253.
(16) Sax, M.; Rodrigues, M.; Blank, G.; Wood, M. K.; Pletcher, J. *Acta Crystallogr.* **1976**, *B32*, 1953.
(17) Jagner, S.; Jensen, B. *Acta Crystallogr.* **1977**, *B33*, 2757.
(18) Svinning, T.; Sörum, H.; *Acta Crystallogr.* **1975**, *B31*, 1581.
(19) Datta, N.; Mondal, P.; Pauling, P. *Acta Crystallogr.* **1980**, *B36*, 906.
(20) Jensen, B. *Acta Crystallogr.* **1982**, *B38*, 1185.
(21) Wilson, K. J.; Derreumaux, P.; Vertoten, G.; Peticolas, W. L. *J. Phys. Chem.* **1989**, *93*, 1351.
(22) Jack, J. J.; Hercules, D. M. *Anal. Chem.* **1971**, *43*, 729.
(23) Culvenor, C. C. J.; Ham, N. S. *J. Chem. Soc., Chem. Commun.* **1966**, *15*, 537.
(24) Cushley, R. J.; Mautner, H. G. *Tetrahedron* **1970**, *26*, 2151.
(25) Partington, P.; Feeney, J.; Burgen, A. S. V. *Mol. Pharmacol.* **1972**, *5*, 269.
(26) Terui, Y.; Ueyama, M.; Satoh, S.; Tori, K. *Tetrahedron* **1974**, *30*, 1465.
(27) Lichtenberg, D.; Kroon, P. A.; Chan, S. I. *J. Am. Chem. Soc.* **1974**, *96*, 5934.

0022-3263/93/1958-1719$04.00/0

Chart I

ACH⁺

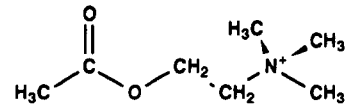

1

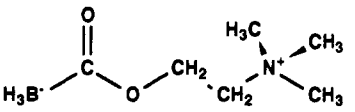

2

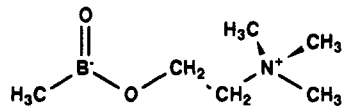

4

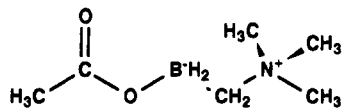

5

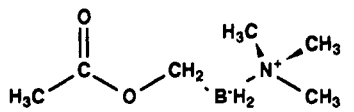

7

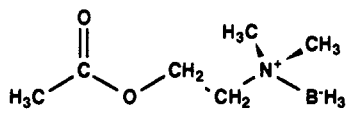

DN10000 workstations. This MNDO version makes use of the Broyden–Fletcher–Goldfarb–Shanno algorithm[30-33] to locate equilibrium geometries on the MNDO potential energy surfaces.

All geometries were calculated using the key word PRECISE, increasing the minimization criteria by a factor of 100. Because the use of a given geometrical input, such as an experimentally-determined crystal structure, favors the conformation associated with that geometry relative to other minima,[34,35] an idealized initial trial geometry (ITG) was used in which all pseudotetrahedral angles were set to 109.5°, all pseudotrigonal angles to 120.0°, and all heavy atom–heavy atom and heavy atom–hydrogen bond distances to 1.5 and 1.1 Å, respectively. All $(3n-6)$ degrees of freedom were allowed to optimize fully from this ITG (with the exception of the two torsion angles used in the preparation of the conformational energy maps, vide infra).

The thermodynamically most stable conformations for each molecule were found by creating a potential energy map on which

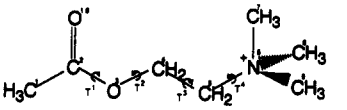

Figure 1. Atomic numbering scheme and major torsion angles for **ACH⁺** and its monoboro-analogs.

was plotted the calculated heats of formation for the conformations defined by the two torsion angles O^3–C^4–C^5–N^6 and C^2–O^3–C^4–C^5, hereinafter referred to as T^3 and T^2, respectively (Figures 1 and 2). The data used in the creation of the maps were obtained using a stepwise method in which T^3 was held constant while T^2 was varied in 10° increments from 0° through 360° while calculating the heat of formation of each incremental conformation, thus creating a "slice" of the heat of formation grid. The torsion angle T^3 was then itself incremented by 10° and the process repeated until a complete 360° by 360° grid of heats of formation was produced. The final grids were plotted using the program SURFER, version 4.11.[36]

Once the conformational minima on the maps were identified, each minimum was reoptimized without constraits. The final geometries thus obtained are the conformational geometries reported herein.

Results

Structural Properties. The conformational energy map for **ACH⁺** is found in Figure 3 with seven minima identified by lower case letters; primed letters indicate that a minimum is related to an unprimed minimum with the same letter by reflection through a plane containing T^3. The final optimized geometry of the most stable conformation of **ACH⁺** (**ACH⁺-a**) in drawn in Figure 4. Table I summarizes the MNDO-calculated structural properties and lists the Boltzmann distribution populations calculated for the minima of **ACH⁺**.

The conformational energy maps for each of the monoboro-analogs of **ACH⁺** are depicted in Figures 5, 7, 9, 11, and 13, with the final optimized geometries of the most stable conformations shown in Figures 6, 8, 10, 12, and 14. The structural properties and Boltzmann distribution populations for these molecules are listed in Table I.

Figures 15a–19a illustrate the calculated bond distances for the most stable conformations for each of the five monoboro-analogs of **ACH⁺** (**1-a**, **2-a**, **4-a**, **5-a**, and **7-a**).

Electronic Properties. Table II summarizes the electronic properties of **ACH⁺** and its monoboro-analogs. The column heading "charge on cationic head" represents the algebraic sum of the MNDO-calculated atomic charges of all atoms directly bound to nitrogen, those hydrogen atoms bound to the atoms directly bound to nitrogen, and the calculated charge on the nitrogen atom itself.[37]

Figures 15b–19b illustrate the heavy atom charge distributions for the thermodynamically most stable conformation of each of the monoboro-analogs of **ACH⁺**.

Discussion

The Structure of ACH⁺. From the atom-labeling scheme of **ACH⁺**, Figure 1, the possible conformations of **ACH⁺** and its monoboro-analogs can be described in terms of four major torsion angles: C^4–C^5–N^6–C^7 (T^4), O^3–C^4–C^5–N^6 (T^3), C^2–O^3–C^4–C^5 (T^2), and C^1–C^2–O^3–C^4 (T^1). However, only T^3 and T^2 were investigated in the present study. The torsion angle T^4 involves rotation about a C–N$(CH_3)_3$ bond and is expected to adopt a nearly trans

(28) Egan, M. A.; Zoellner, R. W. *203rd National Meeting of the American Chemical Society*, San Francisco, CA, 1992, April 5–10, ORGN-15.
(29) Quantum Chemistry Program Exchange (QCPE), Indiana University, Department of Chemistry, Bloomington, IN 47405.
(30) Broyden, L. G. *J. Inst. Math. Appl.* **1970**, *6*, 222.
(31) Fletcher, R. *Comput. J.* **1970**, *13*, 317.
(32) Goldfarb, D. *Math. Comput.* **1970**, *24*, 23.
(33) Shanno, D. F. *Math. Comput.* **1970**, *24*, 647.
(34) Pullman, B.; Courriere, P. *Mol. Pharmacol.* **1972**, *8*, 612.
(35) Gelin, B. R.; Karplus, M. J. *J. Am. Chem. Soc.* **1975**, *97*, 6996.
(36) Golden Software, Inc., 809 Fourteenth St., Golden, CO 80401.
(37) Beveridge, D. L.; Radna, R. J. *J. Am. Chem. Soc.* **1971**, *93*, 3759.

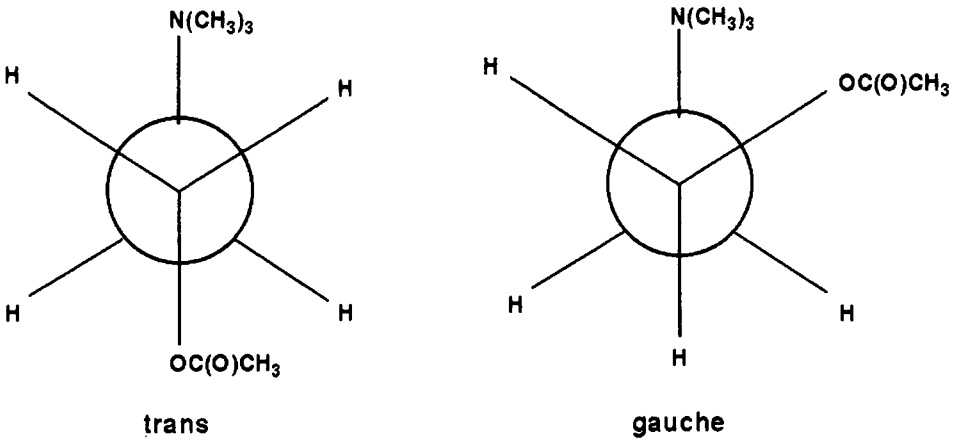

Figure 2. Newman projections of the trans and gauche conformations of ACH^+ about the O^3–C^4–C^5–N^6 (T^3) torsion angle.

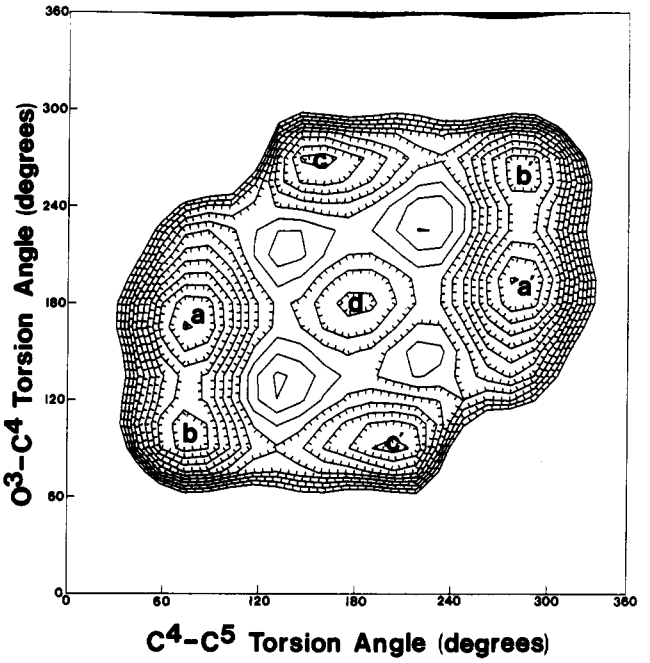

Figure 3. Conformational energy map for ACH^+ with stable conformations identified by letters a–d. Primed letters indicate mirror image conformations of unprimed letters.

conformation (staggered with respect to the rest of the molecule, see Figure 2) based upon steric factors. Thus, T^4 is not expected to influence significantly the overall conformation of the molecule.

The torsion angle T^1, which involves rotation about a bond to a pseudotrigonal carbon atom, is expected to remain nearly planar because of the potentially partial double-bond character of the C^2–O^3 bond, and is expected to have little effect on the overall conformation of the molecule. To test this premise, Radna and co-workers[38] varied T^1 and T^2 while holding T^3 constant at 180°. Three minima were found, each with T^1 = 180.0°. Rotation of T^1 out of the trans-planar conformation involved an increase in energy of up to 20 kcal/mol, and was consistent with partial double bond character in the C^2–O^3 bond.[39]

The orientation of the acetoxy group with respect to the remainder of the molecule is specified by T^2. This torsion angle determines a conformational parameter crucial to biological activity: The distance between the cationic head and the carbonyl oxygen, O^{10}. This distance is important for the molecular interaction with the ACH^+ receptor of ACHase.[40]

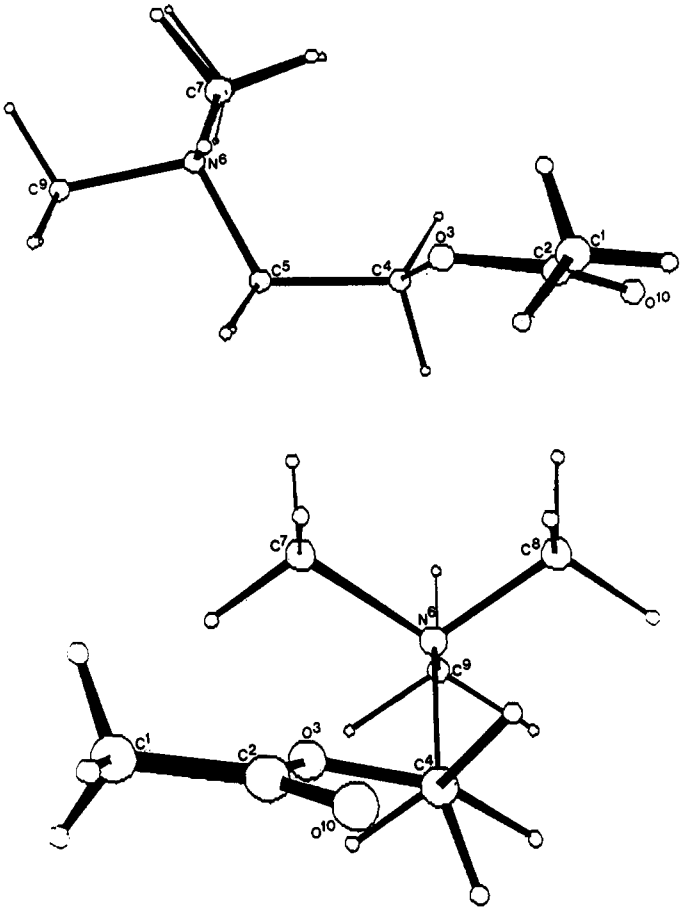

Figure 4. Final optimized geometry of the most stable conformation of acetylcholine (ACH^+-a) as determined by MNDO. Top drawing, view perpendicular to, and bottom drawing, parallel to the C^4–C^5 bond.

Following the example of previous investigators,[37,38,41-44] then, we have used only T^3 and T^2 to describe the conformations of ACH^+ and its monoboro-analogs. (The orientation of T^2 and T^3 in any molecule will be designated by the ordered pair [T^2,T^3]).

(38) Radna, R. J.; Beveridge, D. L.; Bender, A. L. *J. Am. Chem. Soc.* **1973**, *95*, 3831.
(39) Baker, R. W.; Chothia, C. H.; Pauling, P. J.; Petcher, T. J. *Nature (London)* **1970**, *230*, 439.
(40) Wilson, I. B. *Neurology* **1957**, 41.
(41) Liquori, A. M.; Damiani, A.; DeCoen, J. L. *J. Mol. Biol.* **1968**, *33*, 445.
(42) Froimowitz, M.; Gans, P. J. *J. Am. Chem. Soc.* **1972**, *94*, 8020.
(43) Pullman, A.; Port, G. N. J. *Theor. Chem.* **1973**, *32*, 77.
(44) Genson, D. W.; Christoffersen, R. E. *J. Am. Chem. Soc.* **1973**, *95*, 362.

Table I. Structural Information and Boltzmann Distribution Populations for the Acetylcholine Cation and Its Monoboro-Analogs

conformn[b]	torsion angle[a] (deg) T¹ [C²–O³]	T² [O³–C⁴]	T³ [C⁴–C⁵]	T⁴ [C⁵–N⁶]	Boltzmann distribn pop. (%)
ACH⁺-a	7.6	168.7	78.5	178.3	23.41
ACH⁺-a′	352.2	190.4	280.9	181.2	23.41
ACH⁺-b	338.6	96.7	75.9	179.1	14.94
ACH⁺-b′	21.3	263.3	283.3	180.5	14.94
ACH⁺-c	13.7	268.3	153.9	174.5	9.34
ACH⁺-c′	346.3	92.0	206.4	185.5	9.34
ACH⁺-d	359.9	180.0	179.9	180.0	4.51
1-a	209.0	266.8	310.6	192.8	27.49
(1-a′)[c]					27.49
1-b	333.5	200.9	48.6	165.7	22.17
1-b′	26.8	158.2	311.3	194.4	22.17
1-c	195.5	267.4	153.5	174.9	0.34
1-c′	164.0	92.6	206.4	185.3	0.34
2-a	327.2	80.6	47.7	166.1	27.04
2-a′	33.6	279.4	312.1	193.9	27.04
2-b	29.9	240.5	69.5	170.9	21.46
2-b′	331.1	119.3	290.5	189.1	21.46
2-c	14.1	278.4	135.6	177.4	1.50
2-c′	346.0	81.7	224.5	182.7	1.50
4-a	174.2	169.3	64.9	171.1	30.97
4-a′	185.7	191.4	295.6	189.2	30.97
4-b	195.8	139.5	61.4	168.0	13.12
(4-b′)[c]					13.12
4-c	20.2	274.7	135.7	176.3	3.79
4-c′	339.9	85.4	224.4	183.7	3.79
4-d	322.8	84.6	73.3	178.2	2.08
4-d′	37.3	275.1	285.7	181.3	2.08
4-e	359.9	179.8	179.8	179.8	0.07
5-a	6.9	167.4	67.7	173.9	24.80
(5-a′)[c]					24.80
5-b	352.9	191.6	291.6	185.8	24.74
(5-b′)[c]					24.74
5-c	7.9	84.6	225.2	181.8	0.46
(5-c′)[c]					0.46
7-a	1.8	187.1	271.2	177.4	20.29
(7-a′)[c]					20.29
7-b	352.2	93.0	188.0	188.0	13.90
(7-b′)[c]					13.90
7-c	354.6	179.9	180.0	180.0	13.76
7-d	9.4	267.1	269.8	177.2	8.93
(7-d′)[c]					8.93

[a] Torsion angles have been abbreviated so as to include only the two central atoms containing the bond about which the rotational torsion angle is measured. Thus, [C⁴–C⁵] represents the torsion angle defined by atoms O³–C⁴–C⁵–N⁶, [O³–C⁴] represents the torsion angle defined by atoms C²–O³–C⁴–C⁵, and so on. For the monoboro-analogs of ACH⁺, the appropriate atomic substitution is assumed to have been made. The "right hand rule" for assigning the positive direction of rotation has been applied to these angles. [b] Primed conformations are related to unprimed conformations by reflection with respect to T² and T³. [c] This primed conformation was not determined to be a minimum on the MNDO potential energy surface. However, because the unprimed mirror image conformation did optimize fully, the primed conformation was assumed to exist, and the Boltzmann distribution population of the primed conformation was calculated as well.

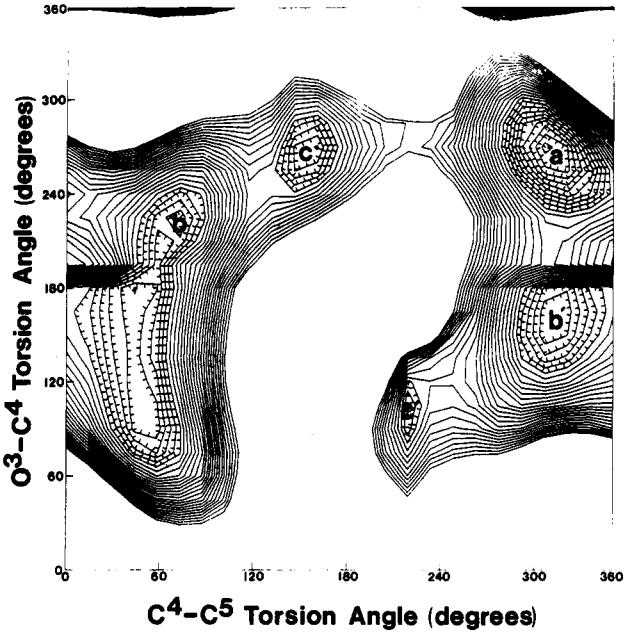

Figure 5. Conformational energy map for 1 with stable conformations identified by letters a–c. Primed letters indicate mirror image conformations of unprimed letters.

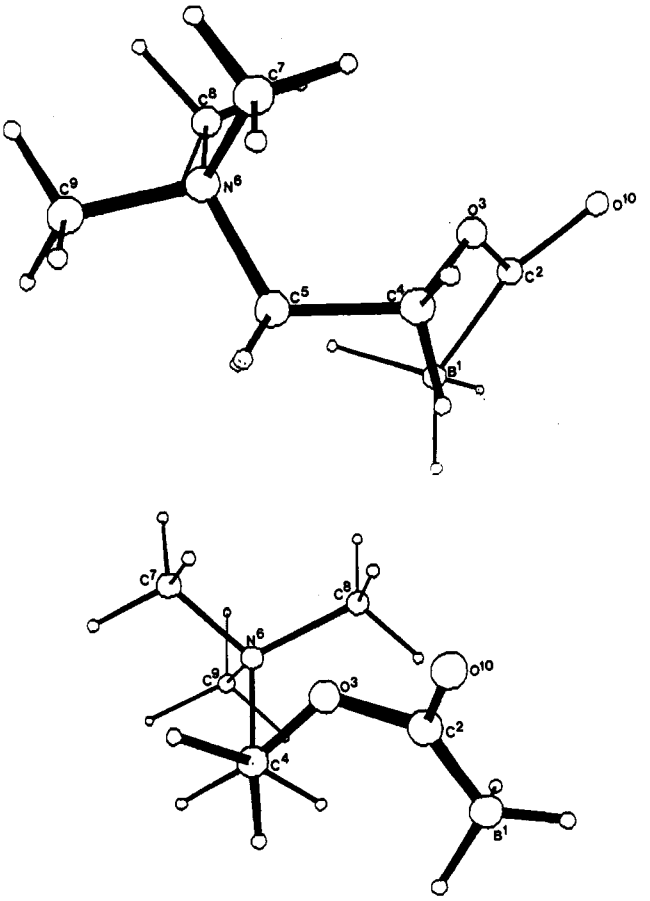

Figure 6. Final optimized geometry of the most stable conformation of 1-boro-acetylcholine (1-a) as determined by MNDO. Top drawing, view perpendicular to, and bottom drawing, parallel to the C⁴–C⁵ bond.

A comparison of the MNDO-calculated bond lengths and bond angles to the most stable conformation of ACH⁺, ACH⁺-a, to experimental crystal structure data is found in Tables III and IV. The crystal structure data vary over a fairly large range, but the MNDO-calculated results for bond lengths and angles are still generally greater than crystal structure data would suggest. However, since theoretical calculations describe molecules in the gas phase without intermolecular interactions, while crystal geometries reflect crystal packing forces and other environmental effects, the MNDO data for ACH⁺ are remarkably consistent with the crystal data.

Table V lists the experimentally-determined conformations about T¹ through T⁴ for ACH⁺ Br⁻, ACH⁺ I⁻, ACH⁺ Cl⁻, and ACH⁺ ClO₄⁻. Choline esters, such as salts

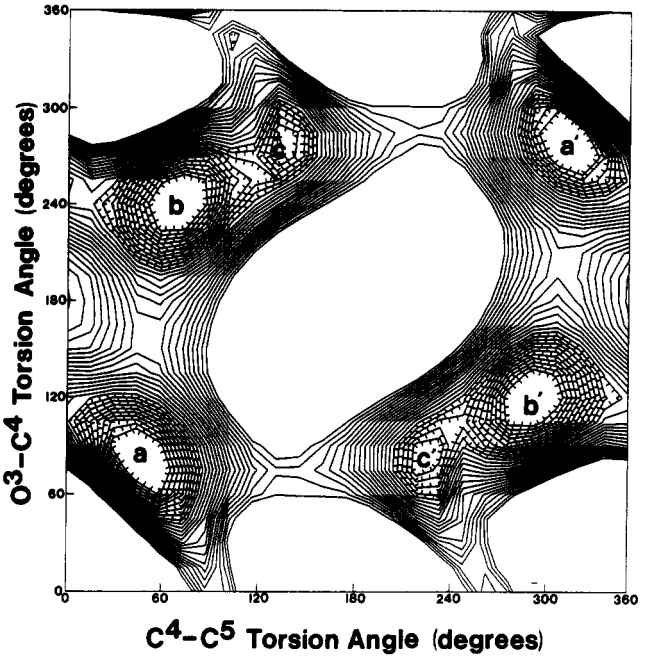

Figure 7. Conformational energy map for 2 with stable conformations identified by letters a–c. Primed letters indicate mirror image conformations of unprimed letters.

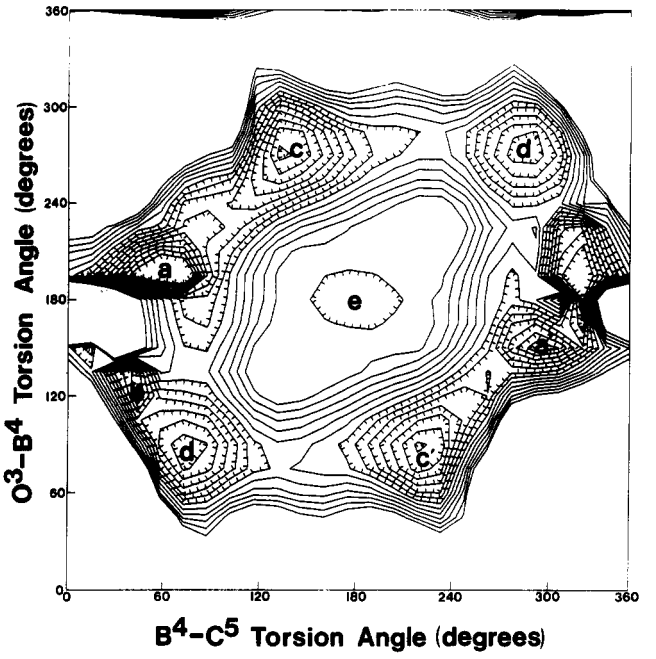

Figure 9. Conformational energy map for 4 with stable conformations identified by letters a–e. Primed letters indicate mirror image conformations of unprimed letters.

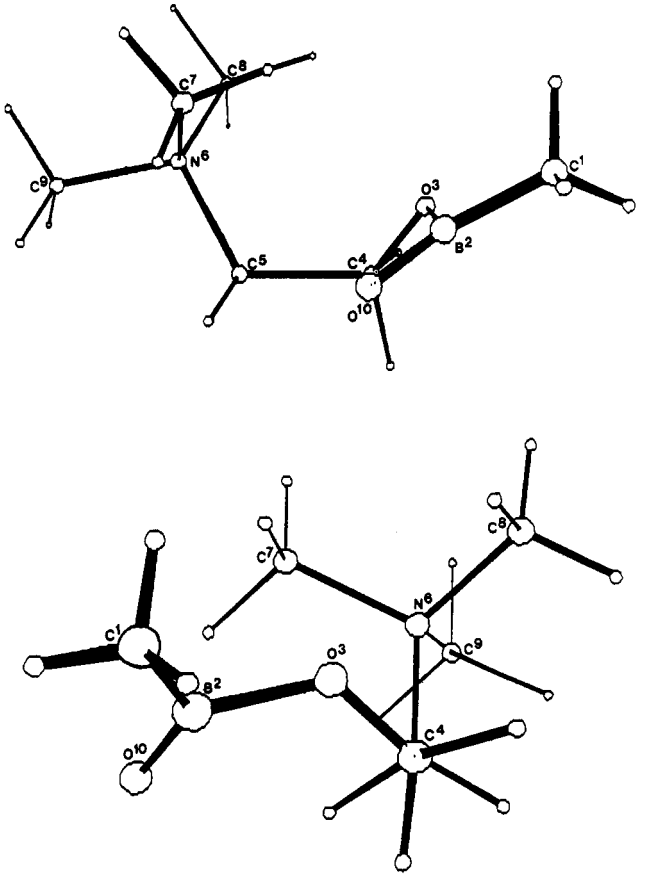

Figure 8. Final optimized geometry of the most stable conformation of 2-boro-acetylcholine (2-a) as determined by MNDO. Top drawing, view perpendicular to, and bottom drawing, parallel to the C^4-C^5 bond.

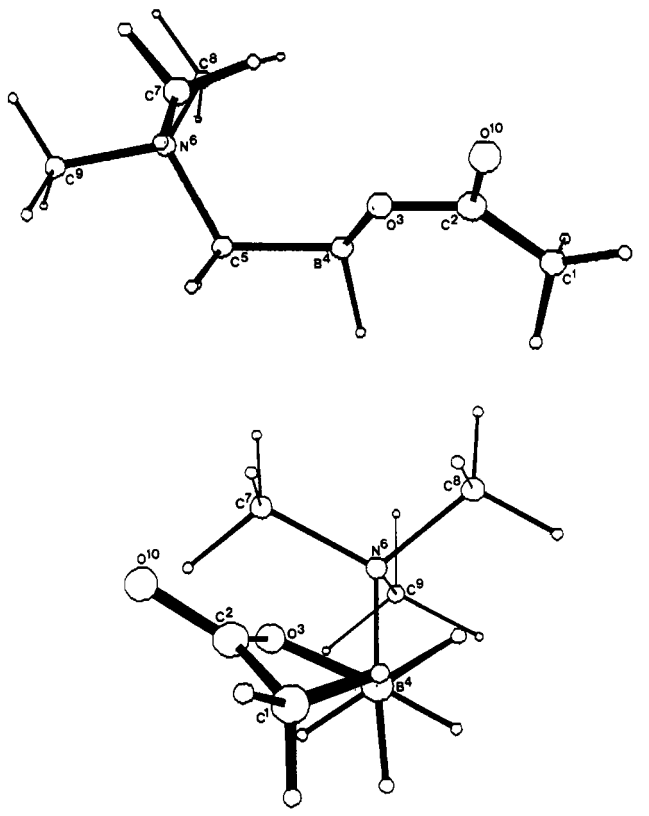

Figure 10. Final optimized geometry of the most stable conformation of 4-boroacetylcholine (4-a) as determined by MNDO. Top drawing, view perpendicular to, and bottom drawing, parallel to the B^4–C^5 bond.

of **ACH$^+$**, are known to adopt different conformations depending upon the environment of the measurement.[14,17] This observation may explain the varying results and geometries obtained in the crystal data reported. The **ACH$^+$ Cl$^-$** and **ACH$^+$ ClO$_4^-$** structures agree with most theoretical studies in which the global minimum energy conformation of **ACH$^+$** is calculated to be trans-gauche about [T^2,T^3]. The gauche-gauche conformation of **ACH$^+$ Br$^-$** and **ACH$^+$ I$^-$** correspond to local minima also found in the theoretical studies.

Table VI summarizes some of the accessible conformations of **ACH$^+$** as determined by various computational methods. The PCILO method used by Pullman and co-

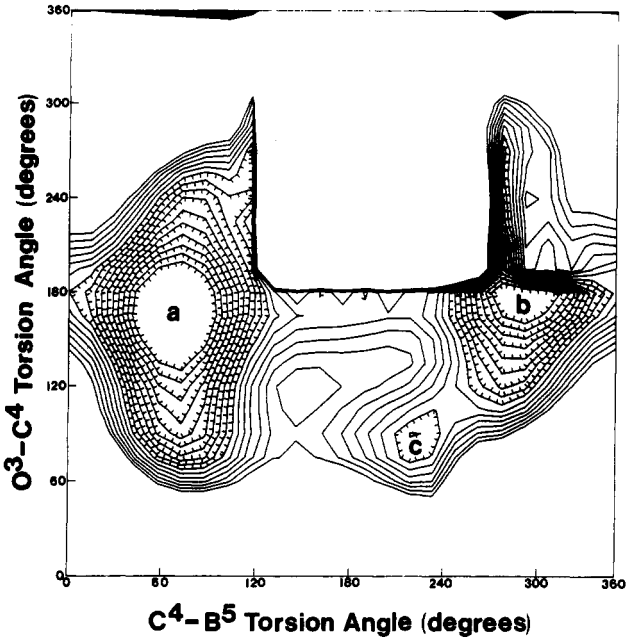

Figure 11. Conformational energy map for **5** with stable conformations identified by letters a–c.

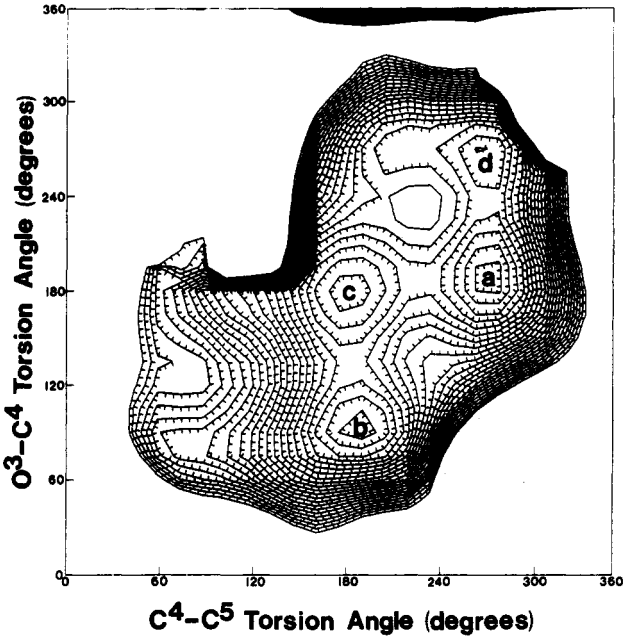

Figure 13. Conformational energy map for **7** with stable conformations identified by letters a–d.

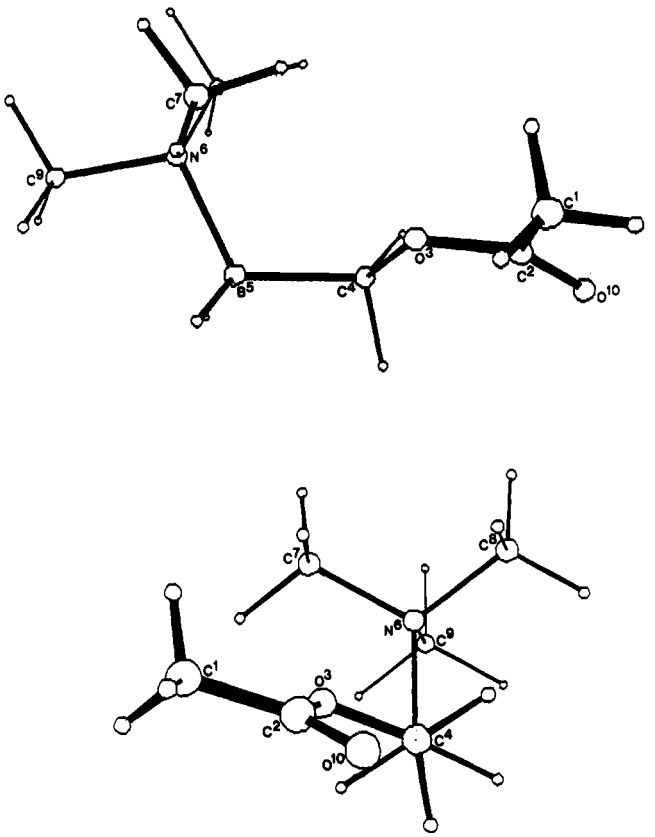

Figure 12. Final optimized geometry of the most stable conformation of 5-boroacetylcholine (**5**-a) as determined by MNDO. Top drawing, view perpendicular to, and bottom drawing, parallel to the C^4–B^5 bond.

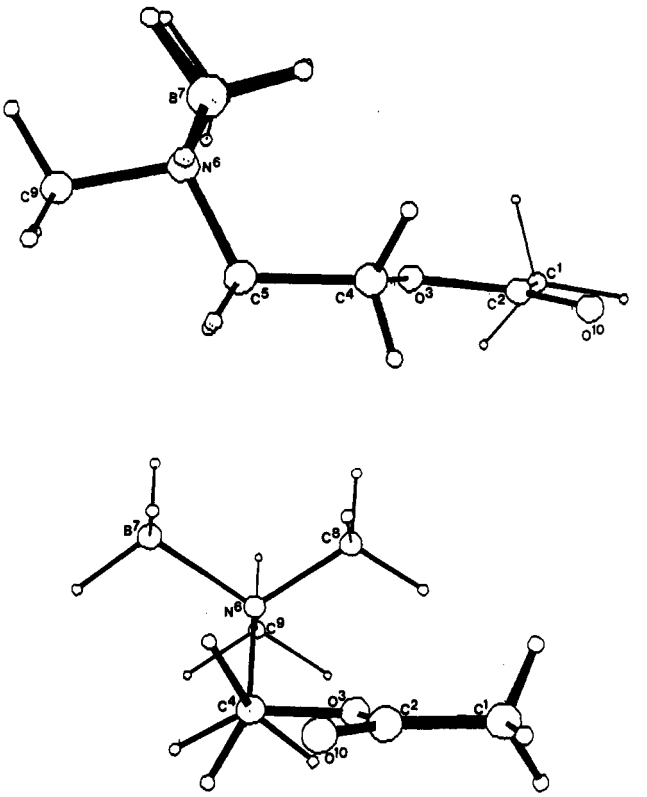

Figure 14. Final optimized geometry of the most stable conformation of 7-boroacetylcholine (**7**-a) as determined by MNDO. Top drawing, view perpendicular to, and bottom drawing, parallel to the C^4–C^5 bond.

workers[45] predicts the global minimum of ACH^+ to occur with $T^1 = T^2 = T^4 = 180°$ and $T^3 = 60°$. This compares favorably with the global minimum predicted by MNDO in the current study ($T^1 = 7.6°$, $T^2 = 168.7°$, $T^3 = 78.5°$, and $T^4 = 178.3°$). In nearly all of the theoretical reports describing the geometry of ACH^+ (Table VI), the trans-gauche conformer ($[T^2,T^3] \approx [180°,80°]$) was found to be the most stable structure. Using classical semiempirical methods, Froimowitz and Gans[42] found the trans-gauche conformer, [185°,75°], to be more stable than the trans-trans conformer, [180°,185°], by 0.46 kcal/mol. Genson and Christoffersen,[44] using an ab initio self-consistent field (SCF) investigation, originally reported that the trans-trans conformer, [180°,180°], was more stable than either of the trans-gauche conformers, [180°,80°] or [180°,60°], by 10 and 19 kcal/mol, respectively. However, a reinves-

(45) Pullman, B.; Courriere, P.; Coubeils, J. L. *Mol. Pharmacol.* **1971**, 7, 397.

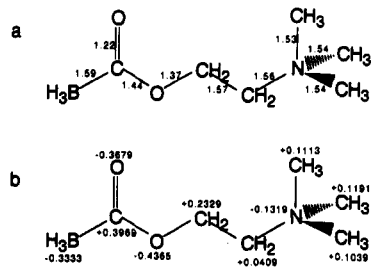

Figure 15. MNDO-calculated bond lengths (a) and heavy atom charge distribution (b) for **1-a**.

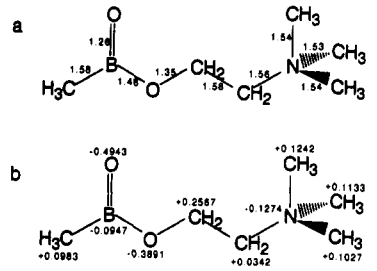

Figure 16. MNDO-calculated bond lengths (a) and heavy atom charge distribution (b) for **2-a**.

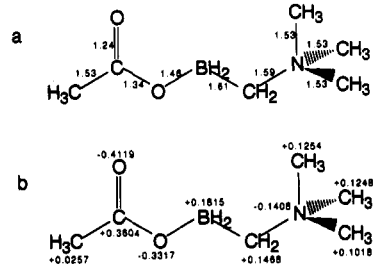

Figure 17. MNDO-calculated bond lengths (a) and heavy atom charge distribution (b) for **4-a**.

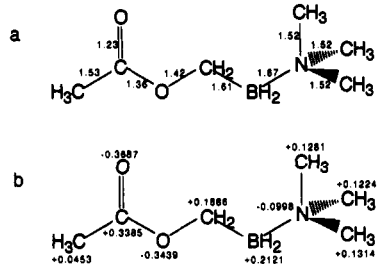

Figure 18. MNDO-calculated bond lengths (a) and heavy atom charge distribution (b) for **5-a**.

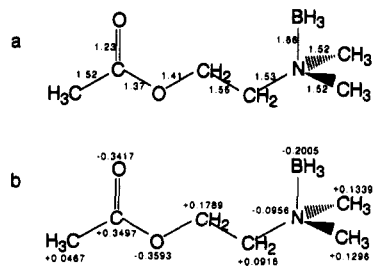

Figure 19. MNDO-calculated bond lengths (a) and heavy atom charge distribution (b) for **7-a**.

tigation of their work by Port and Pullman[46] reported that the trans-gauche conformer was indeed more stable than the trans-trans conformer by about 0.8 kcal/mol.

(46) Port, G. N. J.; Pullman, A. *J. Am. Chem. Soc.* **1973**, *95*, 4059.

Table II. Thermodynamic and Electronic Properties of the Acetylcholine Cation and its Monoboro-Analogs

conformn[b]	heat of formn (kcal/mol)	ionizn potentl (eV)	dipole moment (D)	charge on cationic head[a] (*e*)[c]
ACH⁺-a	98.719	14.646	*d*	0.9109
ACH⁺-a′	98.721	14.645	*d*	0.9110
ACH⁺-b	98.988	14.766	*d*	0.8916
ACH⁺-b′	98.988	14.764	*d*	0.8920
ACH⁺-c	99.269	14.782	*d*	0.8925
ACH⁺-c′	99.269	14.782	*d*	0.8925
ACH⁺-d	99.704	14.528	*d*	0.9137
1-a	−21.597	9.074	18.316	0.8162
1-b	−21.468	9.336	19.260	0.8327
1-b′	−21.468	9.339	19.233	0.8325
1-c	−18.973	8.903	19.645	0.8135
1-c′	−18.973	8.903	19.646	0.8136
2-a	−55.964	7.644	15.044	0.7753
2-a′	−55.962	7.644	15.040	0.7754
2-b	−55.823	7.710	14.821	0.7663
2-b′	−55.824	7.710	14.828	0.7664
2-c	−54.239	7.594	15.938	0.7736
2-c′	−54.239	7.594	15.938	0.7734
4-a	−65.184	9.244	10.742	0.7213
4a-a′	−65.185	9.244	10.726	0.7212
4-b	−64.671	9.292	10.461	0.7133
4-c	−63.933	9.473	9.412	0.7009
4-c′	−63.933	9.474	9.417	0.7009
4-d	−63.576	9.470	10.363	0.6946
4-d′	−63.578	9.468	10.379	0.6946
4-e	−61.524	9.001	12.538	0.7146
5-a	−81.894	10.511	7.333	0.1192
5-b	−81.893	10.514	7.308	0.1131
5-c	−79.512	10.173	5.002	0.0999
7-a	−71.589	11.275	6.910	−0.0273
7-b	−71.363	11.301	5.099	−0.0478
7-c	−71.359	11.294	6.589	−0.0292
7-d	−71.103	11.273	5.469	−0.0431

[a] The algebraic sum of all of the atomic charges within the $-CH_2N(CH_3)_3$ portion of the molecule. For the monoboro-analogs of **ACH⁺**, the appropriate atomic substitution is assumed to have been made. [b] Primed conformations are related to unprimed conformations by reflection with respect to the torsion angles **T²** and **T³**. [c] Calculated charge is reported in fractions of the electron charge, *e*. [d] Undefined for charged species.

Table III. Experimental and Calculated Bond Lengths[a] for the Acetylcholine Cation and Selected Acetylcholine Salts

	ACH⁺				
bond	(Cl^-)[b]	(Br^-)[c]	(I^-)[d]	(ClO_4^-)[e]	**ACH⁺-a**[f]
C^1–C^2	1.49(1)	1.487(6)	1.48(1)	1.51(1)	1.522
C^2–O^3	1.38(1)	1.358(5)	1.37(1)	1.38(1)	1.382
C^2–O^{10}	1.18(1)	1.192(4)	1.20(1)	1.20(1)	1.222
O^3–C^4	1.45(1)	1.452(5)	1.43(1)	1.43(1)	1.399
C^4–C^5	1.47(1)	1.500(5)	1.50(1)	1.47(1)	1.561
C^5–N^6	1.49(1)	1.513(4)	1.53(1)	1.52(1)	1.553
N^6–C^7	1.50(1)	1.496(5)	1.50(1)	1.49(1)	1.542
N^6–C^8	1.49(1)	1.498(6)	1.49(1)	1.51(1)	1.540
N^6–C^9	1.52(1)	1.502(4)	1.52(1)	1.49(1)	1.546

[a] Bond lengths are given in Å with estimated standard deviations in parentheses. [b] Reference 13. [c] Reference 18. [d] Reference 17. [e] Reference 14. [f] This work.

In past theoretical studies, as many as 11 different minima have been found on the **ACH⁺** potential energy surface. With two exceptions,[41,44] the trans-gauche conformation has been found to be more stable than the fully extended trans-trans conformation. However, the magnitude of the energy difference between the trans-gauche and the trans-trans conformers of **ACH⁺** has varied from as little as 0.69 kcal/mol[41] to as much as 3.78 kcal/mol,[38] depending upon the method used. According to Schulman

Table IV. Experimental and Calculated Bond Angles[a] for the Acetylcholine Cation and Selected Acetylcholine Salts

	ACH$^+$				
angle	(Cl^-)[b]	(Br^-)[c]	(I^-)[d]	(ClO_4^-)[e]	ACH$^+$-a[f]
C^1–C^2–O^{10}	129(1)	125.9(4)	127(0.8)	128(1)	128.2
O^3–C^2–O^{10}	123(1)	122.8(4)	121(0.8)	121(1)	118.4
C^1–C^2–O^3	108(1)	111.3(3)	112(0.8)	111(1)	113.4
C^2–O^3–C^4	115(1)	115.7(3)	116(0.8)	115(1)	124.9
O^3–C^4–C^5	111(1)	111.6(3)	111(0.8)	109(1)	109.8
C^4–C^5–N^6	119(1)	116.4(3)	116(0.8)	119(1)	119.1
C^5–N^6–C^7	111(1)	110.7(3)	111(0.8)	109(1)	112.4
C^5–N^6–C^8	111(1)	112.2(3)	110(0.8)	108(1)	111.6
C^5–N^6–C^9	107(1)	107.1(2)	107(0.8)	112(1)	107.2
C^7–N^6–C^9	109(1)	109.8(3)	107(0.8)	110(1)	109.2
C^8–N^6–C^9	111(1)	108.6(3)	112(0.8)	111(1)	108.2
C^7–N^6–C^8	108(1)	108.3(3)	111(0.8)	107(1)	108.1

[a] Estimated standard deviations of bond angles (deg) are given in parentheses. [b] Reference 13. [c] Reference 18. [d] Reference 17. [e] Reference 14. [f] This work.

Table V. Experimentally-Determined Solid-State and MNDO-Derived Conformations of the Acetylcholine Cation

	ACH$^+$				
torsion angle (deg)	(Br^-)[a]	(I^-)[b]	(ClO_4^-)[c]	(Cl^-)[d]	ACH$^+$-a[e]
C^1–C^2–O^3–C^4 (T^1)	4.1	0.0	0.8	5.2	7.6
C^2–O^3–C^4–C^5 (T^2)	78.9	83.0	179.8	193.1	168.7
O^3–C^4–C^5–N^6 (T^3)	78.4	89.0	73.7	84.7	78.5
C^4–C^5–N^6–C^7 (T^4)	175.5	53.0	168.3	171.4	178.3
	gauche-gauche[f]			trans-gauche[f]	

[a] Reference 18. [b] Reference 17. [c] Reference 14. [d] Reference 13. [e] This work. [f] Conformation with respect to T^2 and T^3, respectively.

Table VI. Minimum Energy Conformations of the Acetylcholine Cation As Determined from Other Theoretical Studies

conformational torsion angle (deg)				
C^1–C^2–O^3–C^4 T^1	C^2–O^3–C^4–C^5 T^2	O^3–C^4–C^5–N^6 T^3	C^4–C^5–N^6–C^7 T^4	method
180.0	180.0	180.0	180.0	a
	180.0	60.0		b
	285.0	150.0		c
184.8	171.5	64.6	167.3	d
	70.0	225.0		e
	180.0	180.0	180.0	f
	180.0	60.0	180.0	g
	150.0	60.0		h
	180.0	80.0		i
	100.0	300.0		j

[a] Van der Waals pairwise interactions, ref 41. [b] PCILO (perturbative configuration interaction of localized orbitals), ref 45. [c] Empirical energy functions with INDO (intermediate neglect of differential overlap), ref 35. [d] Ab initio 4-21G gradient relaxation, ref 48. [e] Semiempirical Lennard-Jones 6-12 potentials with point partial charges, ref 42. [f] Ab initio FSGO (floating spherical gaussian orbitals), ref 44. [g] Ab initio SCF (self-consistent field) STO-3G, ref 46. [h] Ab initio SCF/STO-3G, ref 43. [i] EHT (extended Hückel theory), ref 49. [j] INDO, ref 38.

and co-workers,[47] a pharmacologically-active conformation is accessible if the conformation is within 3–4 kcal/mol of the global minimum energy conformation. This amount of distortion energy is easily obtainable from the environment of the molecule and/or from receptor interactions, and should not be sufficient to prevent ACH$^+$ from adopting a trans-trans conformation if required for pharmacological activity.

On the basis of studies of molecular models, it has been suggested[50] that the relative geometries of the cationic head and *ester* oxygen are important determinants of muscarinic activity, while that of the cationic head and *carbonyl* oxygen are important for nicotinic activity. Chothia[51] noted that the geometries of ACH$^+$ which would give rise to nicotinic and muscarinic activity were nearly identical. After experimentation with different C^4- and C^5-substituents on ACH$^+$, it was suggested that the side of ACH$^+$ containing the cationic head, acetate methyl group, and *ester* oxygen on the periphery of the molecule was responsible for muscarinic activity, while the side of the molecule containing the cationic head and *carbonyl* oxygen was responsible for nicotinic activity.[51]

In all experimentally-observed forms of biologically-active ACH$^+$, the T^3 conformation is gauche.[50] The [180°,70°] conformation has been implicated in the nicotinic action of ACH$^+$,[53] and the [180°, −60°] conformation was found in the crystal structure of 1(*R*),2(*S*)-nicotine dihydriodide.[54] The range of conformations [144–213°,60–120°] has been suggested to contain all of the conformations exhibiting the muscarinic action of ACH$^+$,[51] and the [144°,74°] conformation is found in the active form of muscarine as determined by Jellinek.[55] However, Schulman and co-workers,[47] using the MM2 method and ab initio SCF calculations, reported that the conformation of ACH$^+$ in the muscarine pharmacophore was [189°, 132°].

The crystal structure of acetylselenocholine iodide[11] indicates that the conformation about the carbon–carbon bond in the choline residue is trans. This result may explain the markedly different pharmacological activity of acetylselenocholine iodide and its inability to give a positive cholinergic response in electroplax preparations.[56]

The optimal geometry for the hydrolysis of ACH$^+$ by ACHase has been found to be [180°,180°],[57] consistent with the proposed mechanism.[58] A gauche conformation is apparently important if ACH$^+$ is to bind to the cholinergic receptor site but does not effect the ability of ACH$^+$ to act as an ACHase substrate.[11]

In the MNDO-derived geometries of the global minimum conformations of ACH$^+$ and its monoboro-analogs, T^3 is gauche (±47–88°). Sax and co-workers[16] determined the crystal structure of 2,2-dimethylbutyl-3,5-dinitrobenzoate (DMDNB) to test whether, if the quaternary nitrogen atom in ACH$^+$ was replaced by an isoelectronic carbon atom, the resulting molecule would adopt the less sterically hindered trans configuration about T^3. The structural analysis revealed two distinct sites for DMDNB in the crystal: In the first site, the DMDNB ions were exclusively trans, while in the second, the ions were 67% trans and 33% randomly either trans or gauche.

When considering the relative stability of the gauche vs trans conformations of ACH$^+$, it should be noted that ACH$^+$ can be considered a member of a class of 1,2-disubstituted ethanes in which increased stability of the

(47) Schulman, J. M.; Sabio, M. L.; Dish, R. L. *J. Med. Chem.* **1983**, *26*, 817.
(48) Klimkowski, V. J.; Schafer, L.; Scarsdale, J. N.; Alsenoy, C. U. *THEOCHEM* **1984**, *109*, 311.
(49) Kier, L. B. *Mol. Pharmacol.* **1967**, *3*, 487.
(50) Beers, W. H.; Reich, E.; *Nature (London)* **1970**, *228*, 917.
(51) Chothia, C. *Nature (London)* **1970**, *225*, 36.
(52) Sundaralingam, M. *Nature (London)* **1968**, *217*, 35.
(53) Chothia, C.; Pauling, P. *Proc. Nat. Acad. Sci. (Washington, D.C.)* **1970**, *65*, 477.
(54) Koo, C. H.; Kim, H. S. *Daehan. Hwahak. Hwoejee.* **1966**, *9*, 134; *Chem. Abstr.* **1966**, *65*, 6431e.
(55) Jellinek, F. *Acta Crystallogr.* **1957**, *10*, 277.
(56) Mautner, H. G.; Bartels, E.; Webb, G. D. *Biochem. Pharmacol.* **1966**, *15*, 187.
(57) Chothia, C.; Pauling, P. *Nature (London)* **1969**, *223*, 919.
(58) Krupka, R. M.; Laidler, K. J. *J. Am. Chem. Soc.* **1961**, *83*, 1445.

gauche conformation is the norm.[59,60] The stabilization of the gauche conformation of **ACH**$^+$ is thought to involve electrostatic interactions and/or hydrogen bonding between the partially negative ester oxygen (O^3) and a hydrogen atom of one of the three methyl groups of the cationic head.[37,61,62] The close proximity of the quaternary nitrogen (N^6) to the ester oxygen has also been proposed to explain the increased stability of the gauche conformer.[48]

In the current study, three systems, **ACH**$^+$, **4**, and **7**, had gauche conformations which were more stable than trans conformations (Table I). For molecules **1**, **2**, and **5**, no minima which could be considered trans were found. The reason for the increased stability of the gauche relative to the trans conformation remains unclear, as no significant bonding interactions between the ester oxygen and *any* portion of the cationic head was observed. The most stable gauche conformer of **ACH**$^+$, **ACH**$^+$-**a**, for example, exhibited an H^{71}–O^3 distance of 2.76 Å as compared to 4.22 Å for the most stable trans conformer, **ACH**$^+$-**d**. The N^6–O^3 distance in the former was 3.27 Å, while in the latter, the distance was 3.80 Å. Further, MNDO-calculated bond orders for all conformations of **ACH**$^+$ indicated no bonding between the ester oxygen and any of the terminal methyl hydrogens.

At the reduced atomic distances of the gauche conformation, there is opportunity for increased electrostatic interactions between the partially positive *N*-methyl hydrogens and the partially negative ester oxygen. The fact that the trans-trans conformer, **ACH**$^+$-**d**, has a greater positive charge about the cationic head (Table II) than does the trans-gauche conformer, **ACH**$^+$-**a**, and also exhibits a greater negative charge on the ester oxygen (−0.3783 *e* vs −0.3592 *e*) may indicate a slight degree of charge transfer. If so, this charge transfer may be partially responsible for the increased stability of the gauche conformer. Beveridge and Radna,[37] using INDO, found a similar charge redistribution in their [180°,40°] conformer. However, because there was no net change in the charge about the cationic head, these authors concluded that no charge transfer had taken place.

On the basis of X-ray crystallographic analyses,[10,12,13,17,52] NMR studies,[23–25,27,63–66] and Monte Carlo hydration calculations,[67] it has been concluded that the most stable conformation about T^3 is gauche for **ACH**$^+$ in aqueous solution. These latter hydration calculations, however, indicated that relatively free rotation about T^2 is possible. In aqueous solution, **ACH**$^+$ can be described as a positively-charged hdyrated globe with a mobile tail free from interactions with surrounding water molecules.

Other researchers have measured the spectral parameters N and L (the sum and the difference of vicinal coupling constants, respectively) and have translated these NMR parameters into population ratios for the gauche and trans forms of **ACH**$^+$.[27] From such an analysis, it has been calculated[37] that **ACH**$^+$ is approximately 91% gauche and 9% trans about T^3 in aqueous solution. Makriyannis and co-workers,[63] also using NMR techniques, found that **ACH**$^+$ is 100% gauche about T^3 in D_2O and dimethyl sulfoxide, and 97% gauche in $CDCl_3$.

In the ^{1}H-NMR spectrum of **7**, an apparently perfect A_2X_2 system was observed for the $-CH_2CH_2-$ moiety.[1] No observable difference was found in the free energy of the gauche and trans conformers of **7**, and it was concluded that the populations of the two conformers were equal. Further, the barriers to rotation about the C^4–C^5 bond were very small. These results conflict with earlier NMR studies of **ACH**$^+$[23,25–27] in which the population of the gauche conformer was found to be 90–100%. Other researchers[21] believe that the time scale of an NMR measurement is incommensurate with the determination of rapidly changing conformations in these cases, and only a time average of two or more different conformations is actually detected. On the basis of comparisons of solid-state crystal structures and solution-state Raman spectroscopic data, these researchers[21] determined that **ACH**$^+$ in solution exists as two conformations: [160°,300°] and [260°,280°].

MNDO calculations predict that 76.69% of the **ACH**$^+$ conformers will be gauche (46.81% at ±78.5° and 29.88% at ±75.9°), 4.51% will be trans, and 18.68% of the conformers will adopt a staggered conformation (T^3 = 153.9°) neither gauche nor trans (Table I). Apparently, solvent effects must further stabilize the gauche conformers relative to the trans conformer so as to increase the gauche population in solution. However, the results of Makriyannis and co-workers[63] contradict this conclusion, since these researchers found that a high percentage of species adopting the gauche conformation existed in highly-polar D_2O and in less polar solvents such as $CDCl_3$. Solvent effects on the conformation of **ACH**$^+$ cannot be included in MNDO calculations, and comparisons to solution data may not be valid.[68]

Comparisons of the Monoboro-Analogs of ACH$^+$ to ACH$^+$. A detailed understanding of the structures of biological molecules is of paramount importance in establishing physiological function and mechanism. The monoboro-analogs of **ACH**$^+$ which are similar in structure (and charge distribution) to **ACH**$^+$ may also exhibit similar activities in a pharmacological setting.

The **ACH**$^+$ cation (Figure 3) exists primarily in four conformations, denoted by the letters **a** through **d** (and their primed mirror images). With these conformations representing (or approximating) the biologically-important conformations, a comparison may be made to each of the monoboro-analogs of **ACH**$^+$, identifying those analogs which can approximate the conformations of **ACH**$^+$.

The monoboro-analogs **1** and **2** (Figures 5 and 7) can apparently adopt all of the conformations of **ACH**$^+$ except for the fully extended trans-trans conformation. This is presumably due to their high dipole moments, 18–19 and 14–16 D, respectively, and the tendency of molecules to reduce charge separation and, hence, dipole moment, by failing to adopt the much less compact structure of the trans-trans conformation.

The conformation of **1** associated with **ACH**$^+$-**b**, the gauche-gauche isomer **1-a′**, was not calculated to be a stable minimum. However, the mirror image of this conformation, **1-a**, *was* a stable minimum on the MNDO potential energy surface. Thus, the Boltzmann distributions for

(59) Wolfe, S.; Rauk, A.; Tel, L. M.; Csizmadia, I. G. *J. Chem. Soc. B* **1971**, 136.
(60) Wolfe, S. *Acc. Chem. Res.* **1972**, *5*, 102.
(61) Donahue, J. *Structural Chemistry and Molecular Biology*; San Francisco: W. H. Freeman, 1968.
(62) Craven, B. M.; Hite, G. *Acta Crystallogr.* **1973**, *B29*, 1132.
(63) Makriyannis, A.; Sullivan, R. F.; Mautner, H. G. *Proc. Nat. Acad. Sci. (Washington, D.C.)* **1972**, *69*, 3416.
(64) Behr, J. P.; Lehn, J. M. *Biochem. Biophys. Res. Commun.* **1972**, *49*, 1573.
(65) Mautner, H. G.; Dexter, D. D.; Low, B. *Nature (London)* **1972**, *238*, 87.
(66) Cassidei, L.; Sciacovelli, O. *J. Am. Chem. Soc.* **1981**, *103*, 933.
(67) Margheritis, C.; Corongiu, G. *J. Comput. Chem.* **1988**, *9*, 1.
(68) Beveridge, D. L.; Kelly, M. M.; Radna, R. J. *J. Am. Chem. Soc.* **1974**, *96*, 3769.

conformations of 1 were calculated as though 1-a and 1-a′ were both equally populated real minima. The reasons for which MNDO failed to calculate 1-a′ as a stable minimum have not yet been determined. However, the relative distance between the negatively-charged atom B^1 and the cationic head of the molecule appears to be important in this regard, as well as the depth (relatively shallow and flat) of the minimum on the potential energy surface in the vicinity of the assumed position of 1-a′. (These and other possibilities are currently under investigation.)

The conformational energy map of 4 (Figure 9) shows the most similarity to the conformational energy map of **ACH**$^+$. Because of the moderate energy barrier, 2–4 kcal/mol, between the trans-trans conformation and the gauche-gauche and gauche-trans conformations, 4 has only a trace of trans-trans population. This conformation appears, however, to be accessible and the energy difference (approximately 2.4 kcal/mol) should not prevent the molecule from adopting a trans–trans conformation within the active site of **ACHase**.

The conformational energy map of 5 (Figure 11) exhibits significant differences when compared to the conformational energy map of **ACH**$^+$. The map of 5 exhibits no plane of symmetry, and the molecule apparently can only adopt two of the four conformations observed for **ACH**$^+$. The reasons for the absence of a plane of symmetry, and for the lack of primed conformations, are not yet completely clear, as was the case for 1. However, the mirror image conformations were again assumed to exist when calculating the Boltzmann distribution populations for 5.

The conformational energy map of 7 (Figure 13) also shows little evidence of a plane of symmetry. However, this map exhibits a high degree of similarity to the conformational energy map of **ACH**$^+$. Molecule 7 is apparently able to adopt all of the conformations available to **ACH**$^+$, but can only adopt conformations on one side of the plane of symmetry containing the C^4–C^5 bond. As was the case for 1 and 4, no calculated molecular properties were observed which would prevent the primed conformations from being accessible and populated. Therefore, the Boltzmann distributions for 7 were calculated assuming the mirror image conformations existed and were equally populated. If the assumption is then made that all of the mirror image conformations are accessible by 7, only molecules 4 and 7 can adopt all of the conformations available to **ACH**$^+$.

The calculated bond lengths of **ACH**$^+$-a are found in Table III. The 1.38 Å C^2–C^3 bond length is consistent with the double-bond character expected for the ester linkage and is further supported by a p-π to p-π bond order of 0.132. Thus, the assumptions of previous investigators[38,39] concerning this partial double-bond character are supported here.

It is of interest to determine to what extent the interatomic distances of the monoboro-analogs of **ACH**$^+$ differ from **ACH**$^+$. Profound differences in interatomic distances may significantly alter the ability of an otherwise conformationally-correct molecule to bind to a receptor or to fit into the active site of an enzyme such as **ACHase**. From Figures 15a–19a several general trends can be observed. Depending upon the environment of an individual atom, B–C bonds increase from 0.05 to 0.07 Å in length when compared to the corresponding C–C bond in **ACH**$^+$. Boron–oxygen bonds increase from 0.06 to 0.10 Å in length, while B=O bonds increased by 0.04 Å and B–N bonds increased by 0.12 Å in comparison to the C=O and C–N bonds in **ACH**$^+$.

Table VII. Atomic Charge Distributions[a] of Acetylcholine Cation Conformers As Calculated by the INDO, ab Initio, and MNDO Computational Methods

	INDO[b]		ab initio[c]		MNDO[d]	
atom	gauche	anti	conf(1)	conf(2)	ACH$^+$-a	ACH$^+$-d
C^1	−0.047	−0.046	−0.854	−0.855	0.047	0.049
C^2	0.487	0.489	0.565	0.567	0.352	0.357
O^3	−0.288	−0.258	−0.417	−0.423	−0.378	−0.359
C^4	0.195	0.203	−0.306	−0.303	0.181	−0.192
C^5	0.107	0.104	−0.360	−0.361	0.071	0.097
N^6	0.107	0.109	−0.258	−0.257	−0.150	−0.154
C^7	0.120	0.120	−0.615	−0.615	0.118	0.109
C^8	0.121	0.121	−0.604	−0.604	0.108	0.109
C^9	0.120	0.120	−0.627	−0.623	−0.108	0.110
O^{10}	−0.363	−0.369	−0.397	−0.390	−0.306	−0.318
H^{11}	0.041	0.038	0.297	0.312	0.051	0.048
H^{12}	0.036	0.038	0.299	0.288	0.036	0.037
H^{13}	0.012	0.019	0.312	0.305	0.030	0.037
H^{41}	−0.008	−0.012	0.268	0.263	0.026	0.023
H^{42}	0.025	−0.012	0.321	0.313	0.051	0.023
H^{51}	0.022	0.022	0.301	0.301	0.058	0.070
H^{52}	0.024	0.021	0.292	0.307	0.072	0.070
H^{71}	0.030	0.031	0.309	0.308	0.062	0.060
H^{72}	0.037	0.031	0.303	0.304	0.063	0.060
H^{73}	0.028	0.032	0.307	0.308	0.051	0.058
H^{81}	0.032	0.034	0.305	0.306	0.058	0.060
H^{82}	0.033	0.033	0.310	0.309	0.058	0.058
H^{83}	0.033	0.032	0.307	0.307	0.060	0.060
H^{91}	0.032	0.032	0.307	0.307	0.058	0.060
H^{92}	0.031	0.034	0.302	0.309	0.059	0.060
H^{93}	0.032	0.034	0.327	0.319	0.058	0.058

[a] Charges on atoms given in fractions of the electron charge, *e*. [b] The gauche conformer corresponds to a [T^2,T^3] of [60°,180°], ref 38; the anti conformer to [180°,180°], ref 37. [c] Conformation 1, conf(1), corresponds to a [T^2,T^3] of [78.9°,78.4°] and conf(2) to [193.1°,78.4°], ref 67. [d] This work.

In bonds directly involving a boron atom, in addition to significant increases in bond distances, changes in the electronic environment cause neighboring bonds involving oxygen to shorten appreciably. Compared to **ACH**$^+$, the O^3–C^4 bond of 1-a and the C^2–O^3 bond of 4-a are shortened by 0.03 and 0.04 Å, respectively. This is presumably due to the increased negative charge on the oxygen atom in the boron-substituted molecules. It appears that in the substitution of a tetravalent boron atom for a carbon atom significant structural reorganization must be expected.

The charge distribution of **ACH**$^+$ as determined by INDO,[37] ab initio,[67] and MNDO techniques are compared in Table VII. The fundamental differences between INDO and MNDO are evident in the way in which the calculations assign and report electronic charges. The INDO method places a negative charge on the terminal methyl carbon (C^1) while MNDO places a nearly equal but opposite charge on the same carbon. More interesting is the fact that MNDO calculates a negative charge on the quaternary nitrogen atom, while INDO assigns a positive charge to that atom. Both methods are consistent, however, in supporting the idea of charge delocalization over the entire cationic head, with the greater electronegativity of nitrogen resulting in that atom being the least positive site in each case.

The ab initio approach used by Margheritis and Corongiu[67] differs significantly from both MNDO and INDO in the assignment of electronic charges. Like MNDO, the ab initio method assigns the quaternary nitrogen atom a partial negative charge but, unlike MNDO or INDO, also assigns each of the three terminal methyl carbons a significant negative charge. The assignment of electronic charge is largely a function of the method used;

comparisons between different calculational methods are difficult. However, in the current MNDO study it is possible to make direct comparisons between the electronic character of **ACH**$^+$ and its monoboro-analogs because the model and method remain constant. Any significant difference in charge localization between **ACH**$^+$ and its monoboro-analogs can *only* be due to the substitution of an isoelectronic boron atom for a carbon atom.

The monoboro-analogs of **ACH**$^+$ are isoelectronic with **ACH**$^+$ in the sense that each contains the same number of electrons. However, the monoboro-analogs are not (and should not be expected to be) isoelectronic with respect to charge distribution. From the electronic data (Table II) and the heavy atom charge distributions (Table IV) it is evident that **ACH**$^+$ exists as an overall cationic species with a net positive charge about the cationic head. In all conformations available to **ACH**$^+$, a charge about the cationic head of +0.89 to +0.91 *e* is retained.

As would be expected when a neutral carbon atom is replaced by a tetravalent negatively-charged boron atom, a significant redistribution of charge occurs (Figures 15b–19b) in the monoboro-analogs of **ACH**$^+$. As the boron atom is substituted for a carbon atom nearer to the cationic head, the charge on the cationic head diminishes. For biological systems in which a positive charge on the cationic head is important for receptor binding, **5** and **7** may prove to have insufficient receptor affinity, as these molecules are calculated to exhibit the least positive cationic heads. In fact, **7** is calculated to have an overall *negative* charge on the so-called "cationic" head.

None of the monoboro-analogs of **ACH**$^+$, being neutral, can truly be said to resemble the electronic properties of **ACH**$^+$. However, **4** is similar in that, with a moderate dipole moment, approximately 79% of the positive charge on the cationic head exhibited by **ACH**$^+$ is retained by **4**. In contrast, **1** and **2** (Table II) retain a large fraction of the positive charge exhibited by **ACH**$^+$ on the cationic head but also carry a significant dipole moment. Finally, **5** and **7** do not retain the positive charge on the cationic head observed in **ACH**$^+$. Thus, based on these electronic arguments, none of the monoboro-analogs of **ACH**$^+$ mimic **ACH**$^+$, but **4** most closely resembles its electronic character.

The commercially-available **7**, while not the most stable analog, is structurally very similar to **ACH**$^+$ based on the number and geometry of the stable conformations available to it. However, **7** exhibits significant differences in bond lengths and bond angles within the cationic head when compared to **ACH**$^+$. Replacing a carbon atom with a boron atom in the cationic head significantly elongates the N–B bond relative to the N–C bonds and results in 4–5° differences in the associated bond angles.

The most striking change seen in **7** is in the electronic character of the molecule. While **ACH**$^+$ has a net charge about the cationic head of approximately +0.91 *e*, **7** is calculated to have a net charge of –0.028 *e*. Because of the inability of the cationic head to hydrogen bond,[69] and the important role the head plays in binding to the postsynaptic membrane,[70] the forces which are responsible for the binding must largely be a function of the charge about the entire cationic head.[69] The replacement of a carbon atom with a boron atom completely neutralizes the positive charge on the cationic head and thus may significantly alter the ability of the molecule to bind to receptors.

(69) Rosenfield, R. E.; Murrey-Rust, P. *J. Am. Chem. Soc.* **1982**, *104*, 5427.

(70) Michelson, M. J.; Zeimal, E. V. *Acetylcholine, An Approach to the Molecular Mechanisms of Action*; Pergamon Press: Oxford, 1973.

Conclusions

From the MNDO-calculated data presented, we conclude, not surprisingly, that substitution of a carbon atom with a boron atom in **ACH**$^+$ changes the structural and electronic properties of the molecule in ways which are largely dependent upon the site of substitution. From the data presented, **4**, while not the thermodynamically most stable monoboro-analog of **ACH**$^+$, appears to be the most similar analog structurally and electronically. Molecules **1** and **2** most closely resemble **ACH**$^+$ about the cationic head [$-CH_2N(CH_3)_3$] of the molecule, and **5** and **7** most closely resemble **ACH**$^+$ about the acetoxy [$CH_3C(O)O-$] end of the molecule. The monoboro-analog of choice for biological or pharmacological activity, then, depends largely upon which portion of the molecule is involved with the specific activity under investigation, which structural or electronic changes are needed, and finally which pharmacological responses the as-yet-uncharacterized monoboro-analogs of **ACH**$^+$ are expected to produce.

The conformational energy maps for the mono-boro-analogs of **ACH**$^+$ are rather flat, which makes it difficult to exclude the accessibility of any conformations in biological systems. None of the barriers between conformations are greater than about 5 kcal/mol, which is a readily attainable amount of energy from the environment of the molecule or from receptor interactions. Thus, even though the global minimum energy conformations may have no concordance with the conformations necessary for biological activity, other, less stable conformations should be biologically-accessible.

The monoboro-analogs of **ACH**$^+$, if synthesized, may, among other things, find uses as biochemical probes for the study of agonist–receptor binding and biochemical events at the molecular level. Boroanalogs of biological molecules offer significant computational and synthetic interest. We are continuing our studies of boron-substituted analogs of biologically-important molecules using computational techniques.

Acknowledgment. We thank the Northern Arizona University Computer Services for their generous donation of computer resources and the Office of Grant and Contract Services and the Organized Research Committee of Northern Arizona University for their support. This work is a contribution from the Apollo/Hewlett-Packard Undergraduate Computer Project in Computer-aided Molecular Design and Computational Chemistry, Professor Earle B. Hoyt, Jr., Director. We sincerely appreciate the assistance of Professor Roderic Parnell of the Department of Geology of Northern Arizona University, who graciously allowed us to use the SURFER program to construct the conformational energy maps.

Supplementary Material Available: Tables of the torsion angle versus MNDO-calculated heat of formation data used to produce the conformational energy maps of **ACH**$^+$ and its monoboro-analogs, the final MNDO-calculated atomic coordinates for each conformational minimum of **ACH**$^+$ and its monoboro-analogs, and the MNDO-calculated net atomic charge for each atom in each conformational minimum of **ACH**$^+$ and its monoboro-analogs (149 pages). This material is contained in libraries on microfiche, immediately follows this article in the microfilm version of the journal, and can be ordered from the ACS; see any current masthead page for ordering information.